Control system for direct torque controlled and field-oriented controlled drives of permanent magnet synchronous motor

Hau Huu Vo[1,*], *Chau Si Thien Dong*[1], *Dung Quang Nguyen*[1], *Quang Thanh Nguyen*[1], *Trung Van Nguyen*[1], *Duy Hoang Khanh Tran*[1], *Lan Bao Quach*[1], *Liem Dung Phan*[2]

[1]Faculty of Electrical and Electronics Engineering, Ton Duc Thang University, Ho Chi Minh City, Vietnam.
[2]R&P Electronics Company Limited, Ho Chi Minh City, Vietnam.

*Corresponding Author: Hau Huu Vo (Email: vohuuhau@tdtu.edu.vn)
(Received: 14-November-2024; accepted: 17-March-2025; published: 31-March-2025)
http://dx.doi.org/10.55579/jaec.202591.479

Abstract. *This paper focuses on the critical aspect of component selection in designing control systems for field-oriented control (FOC) and direct torque control (DTC) of three-phase permanent magnet synchronous motors (PMSMs). The chosen components significantly influence the performance, efficiency, and reliability of the control systems. Key components include high-speed digital signal processors (DSPs) and microcontrollers (MCUs) for executing complex FOC and DTC algorithms in real-time. Besides that, the selection of insulated-gate bipolar transistors (IGBTs) and metal-oxide-semiconductor field-effect transistors (MOSFETs) is handled according to voltage and switching frequency requirements. Power diodes are crucial for protection against reverse currents, and sensors for current feedback are essential for precise control. Rotor position sensors are particularly vital for both the FOC and the DTC methods to ensure accuracy of motor control applications. Further exploration of these component selections and their impact on FOC and DTC systems will provide valuable insights into the design considerations for motor control.*

Keywords: *Field-Oriented Control, Direct Torque Control, Permanent Magnet Synchronous Motors, Digital Signal Processors.*

1. Introduction

Designing control systems for three-phase permanent magnet synchronous motors (PMSMs) involves careful component selection to ensure optimal performance, efficiency, and reliability [1]. Field-oriented control (FOC) and direct torque control (DTC) are two advanced strategies that require high precision and real-time processing [2–7]. Critical components include high-speed digital signal processors (DSPs) integrated within MCUs, which execute complex algorithms with higher accuracy [8]. The MCUs are often chosen for their ability to integrate multiple features such as ADCs, timers, and communication interfaces, optimizing cost and simplifying system design [9]. The selection between MOSFETs and IGBTs depends on power and switching speed commands: IGBTs suited for higher power loads (up to 1200 V, 400 A, and 20kHz) and MOSFETs preferred for

fast, efficient switching (up to 100kHz) in lower power applications (ratings of $1000V$, $50\ A$) [10]. Power diodes, sensors, and proper cooling mechanisms, such as heat sinks and fans, also play a crucial role in maintaining the long-term reliability of the control system [11]. The FOC and DTC systems performance were enhanced by sophisticated algorithms utilizing predictive control, sliding mode, nonlinear control, search algorithm, fuzzy logic [12–16]. The algorithms require longer computing time in the drive systems. This paper examines the impact of these components on FOC and DTC systems, guiding designers toward more efficient and robust motor control solutions. Next section is mathematical modeling of PMSM, and computation of FOC and DTC drive methods. The third section shows processing time and instruction count for the FOC and DTC methods for a microcontroller, and selection of other related devices. Conclusions are carried out in final section.

2. Mathematical modeling and drives

The fundamental voltage equations governing a PMSM in the natural abc coordinate system are described as follows:

$$u_{sa} = R_s i_{sa} + \frac{d\psi_{sa}}{dt} \tag{1}$$

$$u_{sb} = R_s i_{sb} + \frac{d\psi_{sb}}{dt} \tag{2}$$

$$u_{sc} = R_s i_{sc} + \frac{d\psi_{sc}}{dt} \tag{3}$$

where: u_{sa}, u_{sb}, u_{sc}, i_{sa}, i_{sb}, i_{sc}, ψ_{sa}, ψ_{sb}, ψ_{sc}, represent the phase voltages, phase currents, flux linkages in phases a, b, and c; R_s is the stator resistance. Flux linkages are expressed according to Eqs. 4-6:

$$\psi_{sa} = L_s i_{sa} - L_m(i_{sb} + i_{sc}) + \psi_f \cos(\theta_r) \tag{4}$$

$$\psi_{sb} = L_s i_{sb} - L_m(i_{sa} + i_{sc}) + \psi_f \cos(\theta_r) \tag{5}$$

$$\psi_{sc} = L_s i_{sc} - L_m(i_{sa} + i_{sb}) + \psi_f \cos(\theta_r) \tag{6}$$

where: L_s, L_m represent the self-inductance of each phase, mutual inductance between phases; ψ_f is the flux linkage due to the permanent magnet, θ_r is the rotor position angle. Electromagnetic torque is shown in Eq. 7:

$$T_e = \frac{3}{2} p(\psi_{sa} i_{sa} + \psi_{sb} i_{sb} + \psi_{sc} i_{sc}) \tag{7}$$

where: T_e is the electromagnetic torque; p is the number of pole pairs. Mechanical dynamics equation is written as follows Eq. 8:

$$J_m \frac{d\omega_m}{dt} = T_e - T_L - B_m \omega_m \tag{8}$$

where: J_m is the moment of inertia of the rotor, ω_m is the mechanical angular velocity of the rotor; T_L is the load torque; B_m is the viscous friction coefficient. Two high-performance PMSM drive methods are presented in Figs. 1-2. For both drive methods, Clarke Trans-

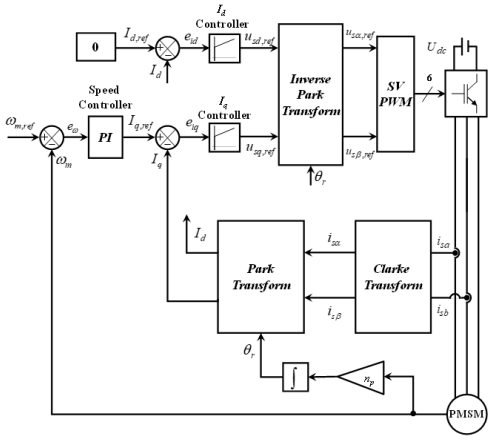

Fig. 1: PMSM drive using FOC method.

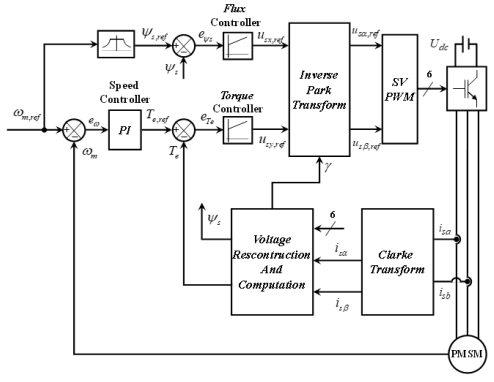

Fig. 2: PMSM drive using DTC method.

form block computes $\alpha\beta$ components of stator current as follows:

$$i_{s\alpha} = i_{sa} \tag{9}$$

$$i_{s\beta} = \frac{i_{sa}}{\sqrt{3}} + \frac{2i_{sb}}{\sqrt{3}} \tag{10}$$

Following equations are implemented in space vector pulse width modulation (SVPWM) block:

$$\overline{U}_{ref} = \sqrt{u_{s\alpha,ref}^2 + u_{s\beta,ref}^2} \tag{11}$$

$$\alpha = \tan^{-1}\left(\frac{u_{s\beta,ref}}{u_{s\alpha,ref}}\right) \tag{12}$$

$$t_a = t_s \sin\left(s_k\frac{\pi}{3} - \alpha\right)\sqrt{3}\frac{\overline{U}_{ref}}{U_{dc}} \tag{13}$$

$$t_b = t_s \sin\left(\alpha - \frac{(s_k-1)\pi}{3}\right)\sqrt{3}\frac{\overline{U}_{ref}}{U_{dc}} \tag{14}$$

$$t_0 = t_s - t_a - t_b \tag{15}$$

where $u_{s\alpha,ref}$ and $u_{s\beta,ref}$ are $\alpha\beta$ components of reference stator voltage vector, t_s is switching period of the SVPWM, $s_k$is an integer, (1 to 6). In case of the FOC, Inverse Park Transform (IPT) block utilizes dq components of reference stator voltage vector and rotor position θ_r to obtain $u_{s\alpha,ref}$ and $u_{s\beta,ref}$

$$u_{s\alpha,ref} = u_{sd,ref}\cos(\theta_r) - u_{sq,ref}\sin(\theta_r) \tag{16}$$

$$u_{s\beta,ref} = u_{sd,ref}\sin(\theta_r) + u_{sq,ref}\cos(\theta_r) \tag{17}$$

For the DTC, in the IPT block, quantities including xy components of reference stator voltage vector$u_{sx,ref}$ and $u_{sy,ref}$ and orienting angle γ, replace for $u_{sd,ref}$, $u_{sx,ref}$ and θ_r, respectively. The I_d and I_q controllers in the FOC are proportional-integral (PI) controllers:

$$u_{sd,ref} = K_{p,d}e_{id} + K_{i,d}\int_0^t e_{id}dt \tag{18}$$

$$u_{sq,ref} = K_{p,q}e_{iq} + K_{i,q}\int_0^t e_{iq}dt \tag{19}$$

where $K_{p,d}$, $K_{p,q}$ and $K_{i,d}$, $K_{i,q}$ are proportional and integral gains of two controllers. The ones are similar to the flux and torque controllers in the DTC. The PI speed controller uses motor speed error e_ω to reference torque-component current $I_{q,ref}$ or reference motor torque $T_{e,ref}$:

$$I_{q,ref} = K_{p,\omega}e_\omega + K_{i,\omega}\int_0^t e_\omega dt \tag{20}$$

where $K_{p,\omega}$ and $K_{i,\omega}$ are proportional and integral gains of the speed controller. The Park Transform block employs $i_{s\alpha}$, $i_{s\beta}$, and θ_r to obtain feedback values of the Id and Iq control loops:

$$I_d = i_{s\alpha}\cos(\theta_r) + i_{s\beta}\sin(\theta_r) \tag{21}$$

$$I_q = -i_{s\alpha}\sin(\theta_r) + i_{s\beta}\cos(\theta_r) \tag{22}$$

For the DTC, the feedbacks are computed by Eqs. 23-27):

$$\psi_{s\alpha} = \int (u_{s\alpha} - R_s i_{s\alpha})\, dt \tag{23}$$

$$\psi_{s\beta} = \int (u_{s\beta} - R_s i_{s\beta})\, dt \tag{24}$$

$$\psi_s = \sqrt{\psi_{s\alpha}^2 + \psi_{s\beta}^2} \tag{25}$$

$$\gamma = \arcsin\left(\frac{\psi_{s\beta}}{\psi_s}\right) \tag{26}$$

$$T_e = \frac{3}{2}p\left(\psi_{s\alpha}i_{s\beta} - \psi_{s\beta}i_{s\alpha}\right) \tag{27}$$

3. Processing time computation and instruction count

The real-time performance of FOC and DTC is significantly influenced by processing speed, memory capacity, and data transmission bandwidth of the controller. A DSP/MCU with high floating-point computation capability, fast sampling rates, and low latency improves control accuracy, minimizes disturbances, and enhances overall system performance. In this section, data processing time and instruction for two described drive methods of PMSM are evaluated on the PIC32MK1024MCM064 microcontroller. The microcontroller, with a 120 MHz clock speed, is capable of handling the computational demands of both drive methods effectively. The instruction counting

is estimated based on general knowledge and experience regarding the control blocks in the FOC system. For a more accurate and scientific estimate, a detailed analysis of each specific block is necessary.

The Clarke and Park Transform blocks typically include operations such as division, multiplication, addition, and trigonometric operations (see Eqs. 9-10), 21-22)). Generally, a Clarke or Park transformation requires about 5-10 basic operations. An approximate estimate of 200-300 instructions for both transformations is made. Estimated instruction counting are 250 instructions with average assumption. Similarly, the IPT block contains calculations for the current and angle, as well as trigonometric operations (see Eqs. 16-17)). This block approximately consumes 200-300 instructions. So it requires 250 instructions in average.

For three PI controllers (see Eqs. 18-20)), one controller typically includes steps such as signals sampling, errors calculating, outputs computing, and adjustments. With three controllers, the total instructions may vary from 150 to 300 instructions, depending on the specific implementation. Average of total value is 225 instructions.

The SVPWM block requires multiple operations to calculate the PWM pulses, including analyzing and generating space vector. (see Eqs. 11-15). This can take about 100-150 instructions. Estimated average instructions are 125 instructions (average assumption).

Factors that are considered consist of sample program, execution time and references. If specific code for transformations or controllers is available, it can provide insights into the actual instruction count. Experiments or data from scientific literature can offer more specific information regarding the actual instruction count required for each part. Studies from existing literature on motor control algorithms can provide more accurate information regarding the required instruction count.

Based on the estimated instruction count, execution time can be calculated for each part. With a clock frequency of 120 MHz, the time per clock cycle is calculated as follows:

$$Time\ per\ cycle = \frac{1}{Frequency} \approx 8.33ns \quad (28)$$

For the FOC system, estimated time for each part (with 5 cycles) are computed in Eqs. (29-32:

$$T_{Clarke\&Park} = Instructions \times Cycles \times Time\ per\ cycle$$
$$T_{Clarke\&Park} = 250 \times 5 \times 8.33ns \approx 10.42\mu s \quad (29)$$

$$T_{IPT} = 250 \times 5 \times 8.33ns \approx 10.42\mu s \quad (30)$$

$$T_{PIControllers} = 225 \times 5 \times 8.33ns \approx 9.37\mu s \quad (31)$$

$$T_{SVPWM} = 125 \times 5 \times 8.33ns \approx 5.21\mu s \quad (32)$$

Total time is calculated as follows:

$$Total\ time = 10.42+10.42+9.37+5.21 \approx 35.42\mu s \quad (33)$$

Actual time is added increase rate 5-50% of total time:

$$Actual\ time = Total\ time \times (1 + Increase\ rate) \quad (34)$$

With an increase rate of 50%, the actual time for the FOC drive system is:

$$Actual\ time \approx 35.42\mu s \times 1.50 \approx 53.13\mu s \quad (35)$$

In case of the DTC system, the flux controller is estimated to consume around 75 instructions, and the inverse transformation approximately 250 instructions, covering current and angle calculations with trigonometric functions. The pulse width modulation requires about 125 instructions for pulse generation and vector synthesis. The torque and speed controllers, performing error calculations and adjustments, are estimated at 150 and 75 instructions, respectively. The coordinate transformation and voltage reconstruction blocks consume about 50 and 125 instructions. Similarly, using a clock cycle time of 8.33 nanoseconds, execution times for each block are calculated as follows (assuming 5 cycles per instruction):

$$T_{Flux\ Controller} = 75 \times 5 \times 8.33\ ns \approx 3.12\ \mu s \quad (36)$$

$$T_{IP\ T} = 250 \times 5 \times 8.33\ ns \approx 10.42\ \mu s \quad (37)$$

$$T_{S\ VPWM} = 125 \times 5 \times 8.33\ ns \approx 5.21\ \mu s \quad (38)$$

$$T_{Torque\ Controller} = 150 \times 5 \times 8.33\ ns \approx 6.25\ \mu s \quad (39)$$

$$T_{Speed\ Controller} = 75 \times 5 \times 8.33\ ns \approx 3.12\ \mu s \quad (40)$$

$$T_{Clarke\ Transform} = 50 \times 5 \times 8.33\ ns \approx 2.08\ \mu s \quad (41)$$

$$T_{Voltage\ Reconstruction} = 125 \times 5 \times 8.33\ ns \approx 5.21\ \mu s \quad (42)$$

The total estimated time is then calculated as:

$$\begin{aligned} Total\ time &= 3.12 \times 2 + 10.42 + 5.21 \times 2 + 6.25 + 2.08 \\ Total\ time &= 35.41\ \mu s \end{aligned} \tag{43}$$

For a more realistic estimate, a 5-50% increase rate is added to account for potential processing overhead:

$$Actual\ time = Total\ time \times (1 + Increase\ rate) \tag{44}$$

With a 50%increase, the actual estimated time becomes:

$$Actual\ time = 35.41\mu s \times 1.50 = 53.12\mu s \tag{45}$$

This approach provides a foundational estimate of the processing time required for the Direct Torque Control system on the microcontroller, with refinements possible through detailed code analysis and experimental validation. With appropriate optimizations, the PIC32MK1024MCM064 microcontroller can process both FOC and DTC algorithms for PMSM within the 100 μs constraint, supporting real-time control at 10 kHz. In order to obtain the efficiency of power conversion devices, the inverter power must be several times greater than the several-kilowatt motor ones in [13] and [16]. So selected power electronic switches are the IGBTs [10], [17]. For FOC and DTC systems, fast recovery diodes are chosen due to roles including freewheeling, protecting against voltage spikes, and supporting commutation. For stator current measurements, the ICs in [18] are proper selections. Commonly-used rotor position sensors include encoders, resolvers, and Hall effect sensors. Encoders offer high accuracy and are suitable for applications requiring precise feedback but are susceptible to electromagnetic interference. Resolvers are robust in harsh environments but require more complex signal processing. Hall effect sensors are cost-effective and easy to integrate but provide lower resolution, making them more suitable for applications with moderate accuracy requirements. For the feedback of precise speed and position in wide-range operation regions, high-resolution incremental rotary encoder can be utilized [7], [13], [19]. This demonstrates the microcontroller's robust capability for both listed motor control applications and sensorless control methods of PMSM drives such as model reference adaptive systems, genetic algorithm, sliding mode observer [20–24]. Simulation and modeling tools such as MATLAB/Simulink, PLECS, and PSIM can be utilized to analyse of the impact of controllers, power devices, control and estimation algorithms on overall system performance. This facilitates optimized design and minimizes potential issues during deployment.

Block diagram of the DSP and microcontroller architecture utilized in the drive system is shown in Fig. 3. The diagram outlines key components, including the CPU, ADC, DAC, QEI, PWM, and CAN FD, which are essential for efficient data acquisition, real-time processing, and high-speed communication. The Fig. 3 illustrates the architecture and integration of these elements within the DSP and microcontroller.

The PIC32MK1024MCM064-I/PT microcontroller is designed for high-performance motor control applications, including DTC and FOC of PMSMs. Its features, such as high-speed ADC, multiple PWM channels, and CAN FD communication, are crucial for precise control and real-time processing. Table. 1 summarizes its key specifications and their relevance to DTC and FOC systems.

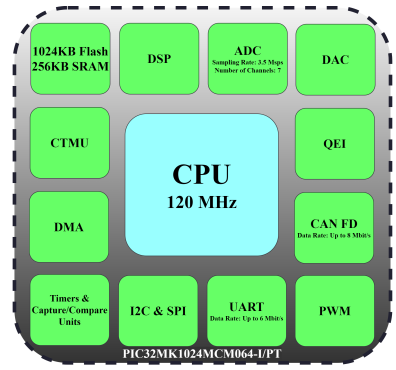

Fig. 3: The PIC32MK1024MCM064-I/PT Architecture.

4. Conclusion

The FOC and DTC methods integrated SVPWM techniques were presented. The PIC32MK1024MCM064-I/PT microcontroller

Tab. 1: Parameters of two controllers.

Feature	Details
Module Name	PIC32MK1024MCM064-I/PT
Flash Memory	1 MB
RAM	256 KB
ADC Channels	7 channels with a sampling rate of 3.5 million samples/second
UART Interface	Supports 6 Mbit/s transmission speed
PWM Channels	Multiple PWM channels for speed, flux and torque control
CPU Frequency	120 MHz
ADC Operation Modes	Continuous and on-demand measurement
Operating Temperature Range	-40^0C to $+125^0$C

is considered as the control system of two drive methods. Its computed processing time is suitable for both methods. The microcontroller is also utilized for advanced motor speed control algorithms or sensorless control techniques. The power IGBTs, diodes, current sensors, encoder are suitable in motor power, switching frequency, command speed range.

5. Acknowledgement

This research is funded by Ton Duc Thang University under grant number FOSTECT.2023.32.

References

[1] F. Korkmaz, I. Topaloglu, M.F. Cakir, , and R. Gurbuz. Comparative performance evaluation of foc and dtc controlled pmsm drives. *roceedings 4th Int. Conf. on Power Eng. Energy Electr. Drives, Istanbul, Turk.*, pages 705–708, 2013.

[2] M. Abassi, . Khlaief, O. Saadaoui, A. Chaari, , and M. Boussak. Performance analysis of foc and dtc for pmsm drives using svpwm technique. *roceedings 2015 16th Int. Conf. on Sci. Tech. Autom. Control. Comput. Eng. (STA), Monastir, Tunis.*, pages 228–233, 2015.

[3] Z. Wang, J. Chen, M. Cheng, and K.T. Chau. Field-oriented control and direct torque control for paralleled vsis fed pmsm drives with variable switching frequencies. *IEEE Trans. on Power Electron.*, 31(3):2417–2428, 2016.

[4] D. Mohanraj, J. Gopalakrishnan, B. Chokkalingam, and L. Mihet-Popa. Critical aspects of electric motor drive controllers and mitigation of torque ripple-review. *IEEE Access*, 10:73635–73674, 2022.

[5] W. Xu, M.M Ismail, and R.Md. Islam. Apermanent magnet synchronous machines and drives. *Flux Weakening Adv. Control. Tech.*, Retrieved from https://www.taylorfrancis.com/books, 2023.

[6] S. Mondal, P. Roy, A. Banerjee, and U. Mondal. A ckf-based sensor-less foc integrated with gh-svpwm for pmsm drives. *Electr. Eng.*, 106(3):3461–3473, 2024.

[7] C.S.T. Dong, H.H. Le, and H.H. Vo. Field oriented controlled permanent magnet synchronous motor drive for an electric vehicle. *Int. J. Power Electron. Drive Syst.*, 14(3):1374–1381, 2023.

[8] V. Pesce, A.Colagrossi, and S. Silvestrini. Modern spacecraft guidance, navigation, and control. *From Syst. Model. to AI Innov. Appl.*, Retrieved from https://www.sciencedirect.com/book, 2023.

[9] Microchip Technology Inc. Pic32mk general purpose and motor control (gpk/mcm) with

can fd family. *https://www.microchip.com/*, 2021.

[10] V. Kumar, R.K. Behera, D. Joshi, and R. Bansal. Power electronics, drives, and advanced applications. *https://www.taylorfrancis.com/books*, 2020.

[11] Z. Zhang, X. Wang, and Y. Yan. A review of the state-of-the-art in electronic cooling. *e-Prime - Adv. Electr. Eng. Electron. Energy*, 1:100009, 2021.

[12] A. Wang, H. Zhang, J. Jiang, D. Jin, and S. Zhu. Predictive direct torque control of permanent magnet synchronous motors using deadbeat torque and flux control. *J. Power Electron.*, 23(2):264–273, 2023.

[13] H.H. Vo. Sliding mode speed controller design for field oriented controlled pmsm drive of an electric vehicle. *J. Adv. Eng. Comput.*, 7(3):164–173, 2023.

[14] T. Nouaoui, A. Dendouga, and A. Bendaikha. Fractional order pid tuned using symbiotic organism search algorithm for field oriented control of the permanent magnet synchronous motor. *Proc. 2023 Int. Conf. on Adv. Electron. Control. Commun. Syst. (ICAECCS), BLIDA, Algeria*, pages 1–5, 2023.

[15] K. Liu and Q. Cheng. Research on new direct torque control strategy of tldmc-pmsm system. *Electr. Eng.*, 105(6):4213–4227, 2023.

[16] H.H. Vo and P. Brandstetter. Modified fuzzy logic pi speed controller with scheduling boundaries of integral time constant for pmsm drive. *Przeglad Elektrotechniczny*, 99(11):175–179, 2023.

[17] STMicroelectronics. Stgwt40hp65fb trench gate field-stop igbt, hb series 650 v, 40 a high speed. *https://www.st.com/*, 2016.

[18] Allegro MicroSystems. Acs724 automotive-grade, galvanically isolated current sensor ic with common-mode field rejection in a small-footprint soic8 package. *https://www.allegromicro.com/*, 2024.

[19] Autonics Corporation. E50s8-3000-3-t-24-cr - 50 mm incremental rotary encoder. *https://www.autonics.com/*, 2024.

[20] P.Q. Khanh and H.P.H. Anh. Novel sensorless pmsm speed control using advanced fuzzy mras algorithm. *Arab. J. for Sci. Eng.*, 47(11):14531–14542, 2022.

[21] M. Kashif and B. Singh. Modified active-power mras based adaptive control with reduced sensors for pmsm operated solar water pump. *IEEE Trans. on Energy Convers.*, 38(1):38–52, 2023.

[22] S.K. Kakodia and G. Dyanamina. Sliding mode mras observer for pmsm-fed electric vehicle control using recurrent neural network-based parallel resistance estimator. *roceedings 2023 IEEE Transp. Electrification Conf. Expo, Asia-Pacific (ITEC Asia-Pacific), Chiang Mai, Thail.*, pages 1–6, 2023.

[23] H.H Boughezala, K. Laroussi, S. Khadar, A. Saad Al-Sumaiti, and M.A. Mossa. Optimized sensorless control of five-phase permanent magnet synchronous motor using a genetic algorithm-real time implementation. *IEEE Access*, 12:98367–98378, 2024.

[24] J. Kong and W. Zhang. A new fast observer-based speed control algorithm for pmsm motor drive based on sliding mode theory. *Int. J. Dyn. Control.*, 12(12):4274–4283, 2024.

About Authors

Hau Huu VO was born in Binh Thuan, Vietnam. He has been working as a Lecturer at Faculty of Electrical and Electronics Engineering (FEEE), Ton Duc Thang University (TDTU), since 2010. He holds a Ph.D. degree from Faculty of Electrical Engineering and Computer Science (FEECS), Technical University of Ostrava (VSB-TUO), Czech Republic in 2017. He has been a member of Modeling Evolutionary Algorithms Simulation and Artificial Intelligence (MERLIN) research group since 2020. His research interests are modern electrical drives.

Chau Si Thien DONG obtained the Ph.D. degree from the FEECS, VSB-TUO, Czech Republic in 2017. She is currently a member of the MERLIN research group. Her research interests focus on modern electrical drives, nonlinear control, adaptive control, robust control, and neural network.

Dung Quang NGUYEN received his MSc degree from Tomsk Polytechnic University, Tomsk City, Russia in 2012. He has published 8 journal papers. His research interests include applications of Kalman filter in control systems; identification and synthesis in fractional, distributed parameter systems.

Quang Thanh NGUYEN has been holding his MSc. degree in Automation and Control Engineering from FEEE, TDTU since 2019. He is preparing to become a Ph.D. student at TDTU. His research interests are applications of intelligent control in electrical drives, microcontrollers.

Trung Van NGUYEN obtained his MSc. degree from Ho Chi Minh City University of Transport, Vietnam in 2020. He is preparing to become a Ph.D. student at TDTU. His research interests include applications of intelligent control in microcontrollers and electrical drives.

Duy Hoang Khanh TRAN has been obtaining the B.Eng. in Automation and Control Engineering from FEEE, TDTU. He is preparing to become MSc. student in field of electrical drives. His research interests are electrical drives and microcontrollers.

Lan Bao QUACH has been obtaining the B.Eng. in Automation and Control Engineering from FEEE, TDTU. He is preparing to become MSc. student in field of electrical drives. His research interests are electrical drives and microcontrollers.

Liem Dung PHAN hold his MSc. degree in Automation and Control Engineering from TDTU, Vietnam in 2019. He is currently Technical Manager at R&P Electronics Company. His research interests are electrical drives and PIC microcontrollers.